

# New Insights to the Sawtooth Oscillation (“ $m/n = 1/1$ mode”) in Hot Plasmas based on High Resolution 2-D Images of $T_e$ Fluctuations

H.K. PARK, N.C. LUHMANN Jr<sup>1)</sup>, A.J.H. DONNÉ<sup>2)</sup>, C.W. DOMIER<sup>1)</sup>, T. MUNSAT<sup>3)</sup>,  
M.J. Van de Pol<sup>2)</sup> and TEXTOR Team<sup>4)</sup>

*Princeton Plasma Physics Laboratory, Princeton University, Princeton, New Jersey, U.S.A*

<sup>1)</sup>*University of California at Davis, California, U.S.A*

<sup>2)</sup>*FOM-Institute for Plasma Physics Rijnhuizen\*, Association EURATOM-FOM, P.O. Box 1207, 3430 BE  
Nieuwegein, The Netherlands*

<sup>3)</sup>*University of Colorado at Boulder, Colorado, U.S.A.*

<sup>4)</sup>*Forschungszentrum Jülich GmbH\*, Institut für Plasmaphysik, Association EURATOM-FZJ, D-52425 Jülich,  
Germany; \*partners in the Trilateral Euregio Cluster*

(Received 5 December 2006 / Accepted 31 July 2007)

Two dimensional (2-D) images of electron temperature fluctuations with high temporal and spatial resolution have been employed to study the sawtooth oscillation ( $m/n = 1/1$  mode) in Toroidal EXperiment for Technology Oriented Research (TEXTOR) tokamak plasmas. 2-D imaging data revealed new physics which were not available in previous studies based on the 1-D electron temperature measurement and X-ray tomography. A review of the physics of the sawtooth oscillation is given by comparative studies with prominent theoretical models and suggests that a new physics paradigm is needed to describe the reconnection physics of the sawtooth oscillation. The new insights are: A pressure driven instability (not a ballooning mode) leads to the “X-point” reconnection process. The reconnection process is identified as a random 3-D local reconnection process with a helical structure. The reconnection time scale is similar for different types of sawtooth oscillation (“kink” and “tearing” type) and is significantly faster than the resistive time scale. Heat flow from the core to the outside of the inversion radius during the reconnection process is highly collective rather than stochastic.

© 2007 The Japan Society of Plasma Science and Nuclear Fusion Research

Keywords: sawtooth, magnetic reconnection, electron cyclotron emission imaging

DOI: 10.1585/pfr.2.S1002

## 1. Introduction

Technology advances in mm-waves and signal processing have enabled the development of a microwave “camera” system [imaging system] which can provide high time resolution 2-D images of electron temperature fluctuations. 2-D images of the electron temperature fluctuations measured by an electron cyclotron emission imaging (ECEI) system [1] have been used to study the physics of the sawtooth oscillation (“ $m/n = 1/1$ ”) in TEXTOR. The sawtooth oscillation common in tokamak plasmas, while benign in moderate beta plasmas, is potentially harmful in future fusion grade plasmas [2], if the growth of this mode is not controlled. In order to identify the control mechanism(s), it is thus imperative to have a better understanding of the underlying physics of the sawtooth oscillation. The observed 2-D ECE images are directly compared with the predicted 2-D pattern of the prominent theoretical models for the sawtooth oscillation: the *full reconnection* [3, 4], *quasi-interchange* [5], and *ballooning mode* [6, 7] models.

The time evolution of the growth/decay of the island/hot spot before the crash and the heat flow pattern after the crash resembles that of the *full reconnection model*; however, the reconnection process is not helically symmetric and the crash time is not even close to the resistive time scale. The fact that the time evolution of the 2-D images of the hot spot/island observed at the high field side does not resemble those from the *quasi-interchange model* suggests that pressure driven instabilities are dominant over magnetic instabilities for the crash mechanism of the sawtooth oscillation. The image of the initial reconnection process at the low field side is similar to the pressure driven instability of the *ballooning mode model*; however, the similar crash pattern argues against this model. Here, the global stochasticity of the magnetic field line may not be the dominant mechanism for the transport of the core heat, since the heat transfer is highly collective during the reconnection time. The earlier 3-D localized reconnection model [6, 7] based on the ballooning mode only inhibits in the lower field side. Further analysis of the crash pattern employing the plasma rotation clarifies that the crash pattern is toroidally local-

author's e-mail: park@pppl.gov

ized and has no preferred spatial location along the inversion radius. Other types of pressure driven modes such as the interchange mode should be considered as candidates for the reconnection of the sawtooth oscillation.

## 2. Electron Cyclotron Emission Imaging (ECEI) Systems on TEXTOR

In magnetized plasmas, the electron gyro motion results in emission of radiation at the electron cyclotron frequency and its harmonics  $\omega_{ce} = eB/m_e$ , where  $B$  is the applied magnetic field strength,  $e$  is the electron charge, and  $m_e$  is the electron mass. In optically thick plasmas where the electron density and temperature are sufficiently high, the radiation intensity approaches that of black body emission where the intensity is directly proportional to the local electron temperature. In tokamak plasmas, the ECE frequency has a spatial dependence due to the radial dependence of the applied toroidal magnetic field  $B(R) = B_o R_o/R$ , where  $R_o$  and  $B_o$  are the geometric center and the magnetic field strength at the center of the plasma, re-

spectively. The fundamentals of the ECE process are well established and have been routinely utilized to measure local electron temperatures in fusion plasmas [8, 9]. In a 2-D electron cyclotron imaging (ECEI) system, the single antenna of a conventional 1-D radiometer is replaced by an array of antennas as shown with the optical design of the system in Fig. 1. Here, large collection optics are required to project high resolution images of the local electron temperature emission onto sensitive 1-D arrays through advances in array technology with well defined antenna patterns and state-of-the-art wide band radio frequency (RF) and intermediate frequency (IF) electronics as described in detail in Ref [10].

A prototype system [1] has been developed for the TEXTOR tokamak plasma. The system has 16 (vertical)  $\times$  8 (horizontal) sampling volumes arranged in a 2-D matrix of 16 cm (vertical)  $\times$  7 cm (radial) with a time resolution of  $\sim 5 \mu\text{sec}$ . The fluctuation quantities are relatively calibrated to the averaged value obtained with a long integration time and the intensity of the images is represented by  $\delta T_e / \langle T_e \rangle$ , where  $T_e$  is the electron temperature and  $\langle \rangle$

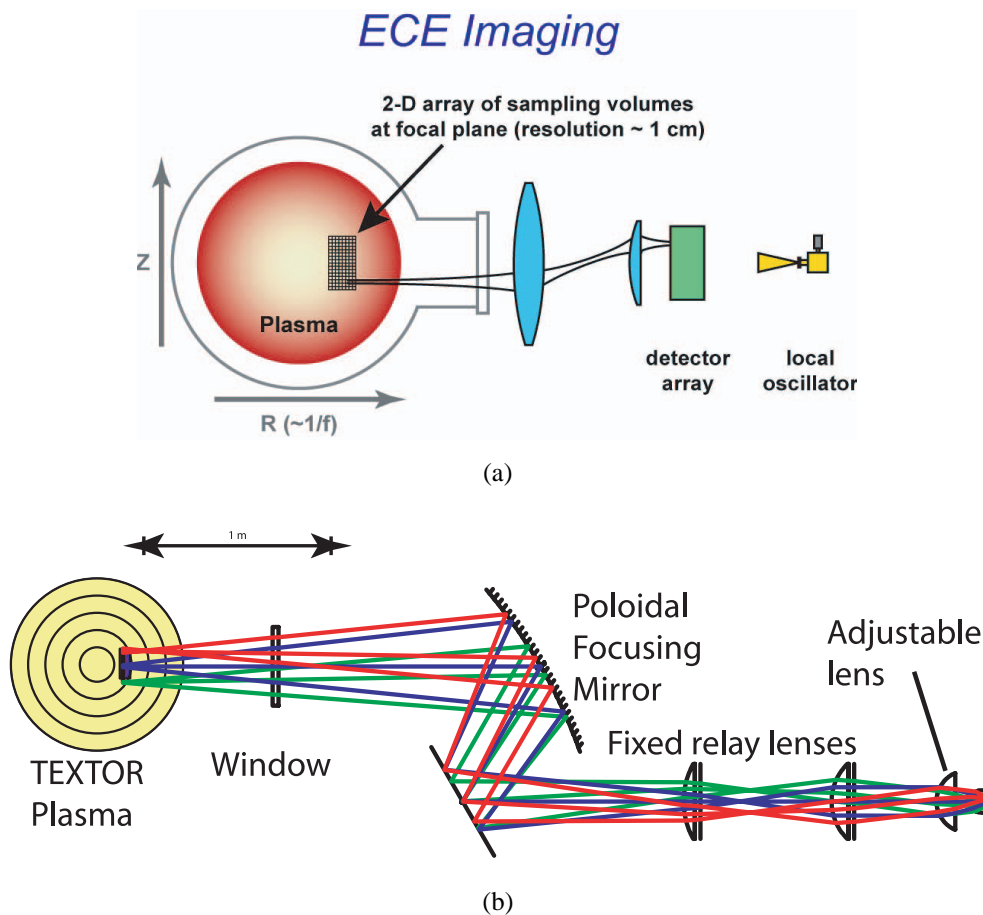


Fig. 1 (a) Conceptual schematic of the microwave camera system on TEXTOR where the vertical sample volume is imaged on the 1-D array (b) Optical design of the Microwave imaging system where the focal depth is controlled by the adjustable lens so that the images can be measured at various locations along the horizontal plane. The target plasma is concentric and magnetic field strength falls as function  $(1/R)$ . The left half of the plasma in Fig. (a) with the smaller  $R$  is the high field side and that with the larger  $R$  is low field side.

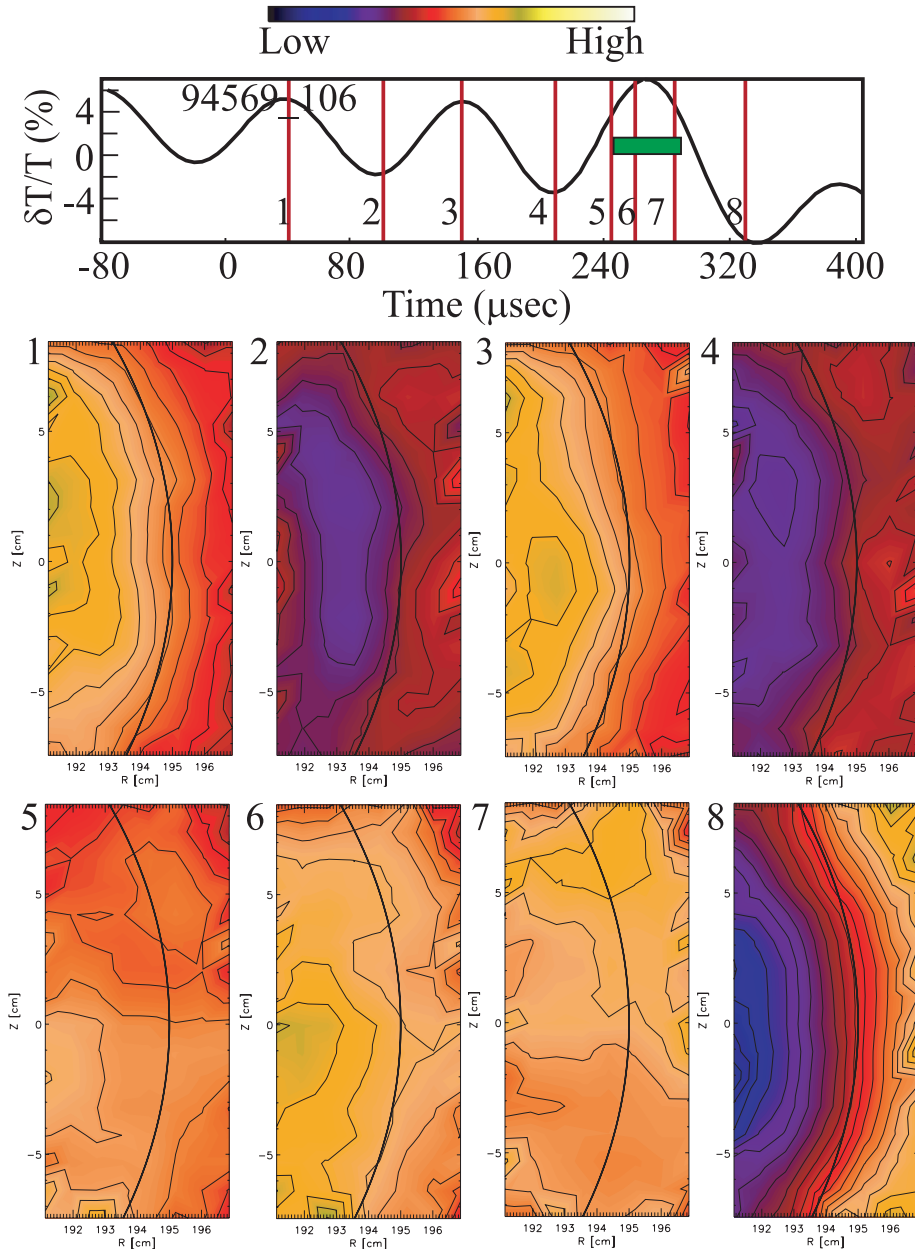


Fig. 2 Illustration of the evolution of the island (blue color) and  $m/n = 1/1$  mode (yellowish green color) during precursor time is given in frames 1 to 4. The distortion of the  $m/n = 1/1$  mode is an indication of the initiation of the reconnection due to the pressure driven mode as shown in frames 5-7. The island is fully recovered after the crash (frame 8). In this case, the plasma rotation speed is estimated as  $\sim 8 \times 10^4$  m/sec.

is the time average. Diamagnetic and poloidal effects are negligible in this experiment.

### 3. Experimental Results

The TEXTOR tokamak plasma has a circular shape with a major radius of 175 cm and a minor radius of 46 cm. The range of toroidal magnetic field in the present work was 1.9-2.4 T and the corresponding plasma current was  $< 305$  kA. The  $H^+$  plasma is heated with energetic neutral beams ( $D_0$ ,  $\sim 50$  keV, up to 3 MW) in order to maximize the temperature fluctuation of the sawtooth oscillation as well as to control plasma rotation (by varying the ratio of co-

to counter injection with respect to the direction of plasma current. The key plasma parameters were as follows: the central electron density and temperature range from  $1.5$  to  $2.5 \times 10^{19} \text{ m}^{-3}$  and from  $1.2$  to  $1.6$  keV, respectively. The corresponding peak toroidal beta is  $\sim 1.0\%$  and the average poloidal beta is between  $0.3$  and  $0.5$ . The toroidal rotation of the plasma varied from  $\sim 1 \times 10^4$  m/s to  $\sim 8 \times 10^4$  m/s. The speed of a thermal electron is  $\sim 6 \times 10^7$  m/s. The Alfvén and ion acoustic speeds are  $5 \times 10^6$  and  $7 \times 10^5$  m/s, respectively. Using plasma parameters close to the inversion radius, the calculated characteristic reconnection time ( $\tau_c = \sqrt{\tau_A^* \tau_r}$ ) is  $\sim 700 \mu\text{s}$ , where  $\tau_A^*$  is the Alfvén time near the inversion radius and  $\tau_r$  is resistive time.

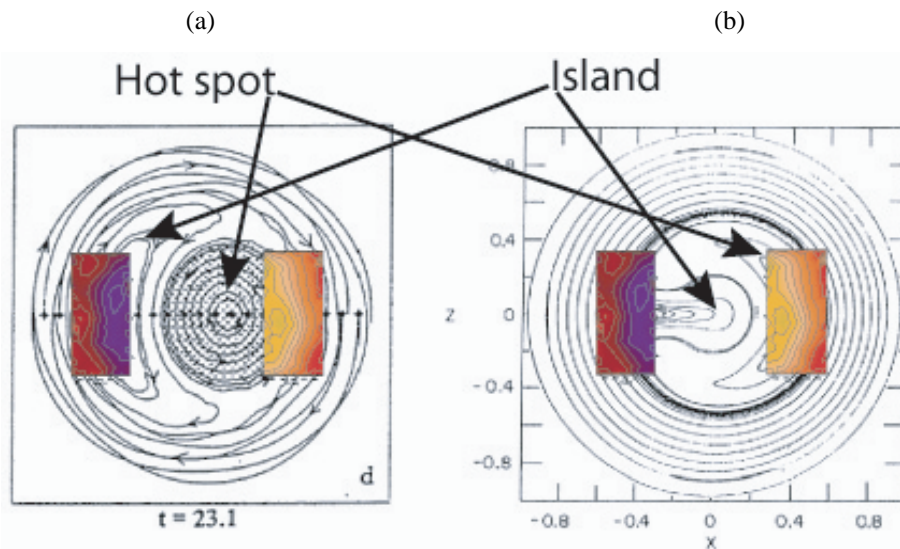


Fig. 3 Direct comparison of the 2-D image of the island (cold spot as shown in blue) and  $m = 1$  mode (hot spot as shown in yellowish color) with the simulation result from (a) the full reconnection mode (by Kadomtsev) and (b) quasi-interchange model (by Wesson). The pattern appears in good agreement with the full reconnection model but grossly disagrees with the quasi-interchange model. Color scale is the same as in Fig. 2.

In Fig. 2, the growth of the island and evolution of the hot spot in the fast rotating plasma are characteristics of the tearing type instability proposed by the full reconnection model where the presence of the island (precursor) is an indication of the occurrence of the helically symmetric reconnection process (i.e., development of the  $m = 1$  mode from  $m = 0$  mode for  $n = 1$ ). In this model, the heat from the  $m = 1$  mode and cold plasma from outside the inversion radius is exchanged through an elongated current sheet similar to the Sweet-Parker model as illustrated in earlier simulation based on single MHD fluid model where the hot spot diminishes as the island is fully occupied through a long reconnection time (resistive time scale). This is contrast to the fact that there is no clear indication of the heat exchange until the distortion of the  $m = 1$  mode is developed as shown in frames 5 to 7. The observed distortion of the  $m = 1$  mode resembles the “pressure finger” proposed by the ballooning mode model when the plasma beta is moderate ( $\beta_t \sim 1\%$  and  $\beta_p \sim 0.4$ ). After the crash, while the stable region (island) is fully occupied, the post-cursor was observed and it is identified as  $m = 0$  mode. In the ballooning mode model, the finite pressure effect develops a pressure bulge at the low field side and eventually leads to the ballooning mode as the pressure gradient increases. Note that there will be no pressure bulging and ballooning modes at the high field side due to the total flux conservation. A striking observation of a similar reconnection process at the high field side of the inversion radius concludes that the cause of the reconnection is not due to a pure ballooning mode. A variety of experimental measurement of 2-D ECE images provided an opportunity to compare the measured 2-D images with the predicted 2-D pattern of the prominent theoretical models for the sawtooth oscil-

lation [11–13]: the *full reconnection*, *quasi-interchange*, and *ballooning mode* models. The pattern of the island and hot spot obtained during the precursor oscillation provide an opportunity to directly compare the shape of the island and hot spot with the expected simulation results from the full reconnection and quasi-interchange models as illustrated in Fig. 3. For the tearing type of the sawtooth oscillation, the growth of the island that is evident in the 2-D image through the plasma rotation (appears as a precursor) is an indication of the occurrence of the reconnection in the full reconnection model. The fact that there is no clear heat flow prior to the presence of the pressure finger which leads to the puncture of the magnetic field, suggests a different (or modified) reconnection process for the full reconnection model. In the course of this study, two types of the sawtooth oscillation were observed; “tearing type” and “kink type” and the time scale of the growth of the pressure finger and reconnection process for both the kink and tearing type.

The heat flow pattern during the reconnection process following the pressure finger is observed to be highly collective and the flow pattern outside the inversion radius indicates that accumulation of the heat is symmetric within the so called “mixing zone” before propagating radially. After the relatively long growth time of the island ( $\sim 1.5$  ms), the  $m = 1$  mode enters into the crash phase. 2-D images of the initial crash phase at both the high and low field side are directly compared with the simulation results of the *ballooning mode model* from the plasma with a similar poloidal and toroidal beta as illustrated in Fig. 4. The distortion of the sawtooth oscillation, just before the crash time, occurs in the form of a “pressure finger”, reminiscent of the ballooning mode accompanied with the finite

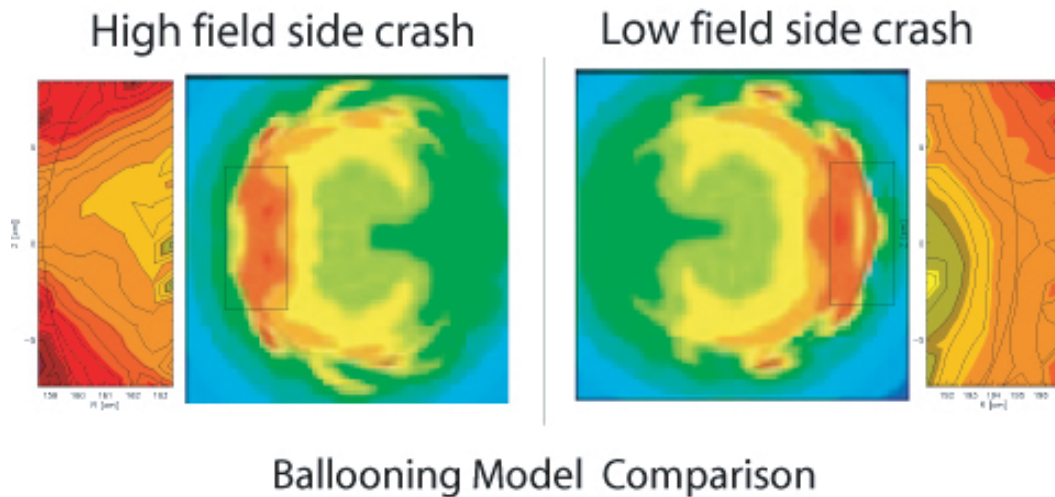


Fig. 4 Direct comparison of the 2-D image of the distorted sharp pressure point which leads to the reconnection with those from simulation is shown. The “pressure finger” of the ballooning mode model (rectangular box in the simulation) at the low field side is in good agreement with the measured 2-D image (far right) but the observed pressure point at the high field side (far left) is inconsistent with that of the ballooning mode model (rectangular box in the simulation). Color scale is the same as in Fig. 2.

pressure effect [14].

In plasmas with a moderate beta ( $\beta_p \sim 0.4$  and  $\beta_t(0) \sim 1\%$ ), where the experiments were performed, the level of the ballooning modes and global stochasticity of magnetic field lines that are strongly coupled with the pressure surfaces, is moderate compared to those in high beta plasmas in the ballooning mode model. The sharp point of the pressure finger eventually leads to the puncture of the magnetic field near the inversion layer and the exhaust of the heat occurs in a coherent manner through the poloidally localized hole in the inversion radius similar to the case of a broken water dam. The observation of the crash at the high field side clearly suggests that this mode is pressure driven, but not necessarily a ballooning type mode. Furthermore, the global stochasticity of the magnetic field may not be the dominant mechanism for the transport of the core heat, since the heat ejection pattern is high collective. The time evolution of the growth/decay of the island/hot spot before the crash and the heat flow pattern after the crash resembles that of the *full reconnection model*. The fact that the time evolution of the 2-D images of the hot spot/island does not resemble those from the *quasi-interchange model* suggests that pressure driven instabilities are dominant over magnetic instabilities for the crash mechanism of the sawtooth oscillation. In the *full reconnection model*, the extent of the reconnection zone is poloidally localized and the finite poloidal opening is helically symmetric along the  $q = 1$  surface so that the current density within the  $m = 1$  mode is removed through the reconnection process. The change of the central current density before and after the crash has been the fundamental of the full reconnection model. However, the measured central  $q$  value inside the  $q = 1$  surface did not change significantly from the value before the crash [16, 17]. This discrepancy invoked many different

theoretical models. In the ballooning mode model, such discrepancy has been eliminated by introducing a global magnetic field stochasticity concept so that the core plasma current does not have to change while the core heat can be dispersed rapidly. In the previous section, the comparison study with the ballooning mode model indicated that the pattern of the heat transfer during crash time is highly coherent rather than stochastic.

The earlier 3-D localized reconnection model [15] based on the ballooning mode predicted that the localized opening along the helical structure on the toroidal plane is always localized in the low field side due to the nature of the ballooning mode. In order to determine whether the reconnection zone is helically symmetric or helically localized, at least two imaging systems separated toroidally are required. The alternative is to utilize the time of flight method based on the plasma rotation that can be controlled by the momentum of the heating beam sources. In the rotating plasma, the time evolution of 2-D images (radial and poloidal view) is equivalent to an extended view along the toroidal direction. Here the data are from the same plasma parameters and there is relatively small variation in rotation speed estimated based on precursor. As illustrated in Figs. 2 and 5, the precursor oscillation provides the time scale of the plasma rotation speed which is  $\sim 8$  and  $7 \times 10^4$  m/sec (toroidal circumference is  $\sim 10$  m), respectively. The time evolution of the island and hot spot prior to the crash time in Fig. 5 is quite similar to the images shown in Fig. 2. However, the reconnection occurred after the last view of the island (frame 3) and partial images of the reconnection zone in the lower part of the viewing window was captured in Fig. 5 whereas the whole reconnection process was captured in Fig. 2. The crash time is defined as the initial time when the first heat is detected outside of

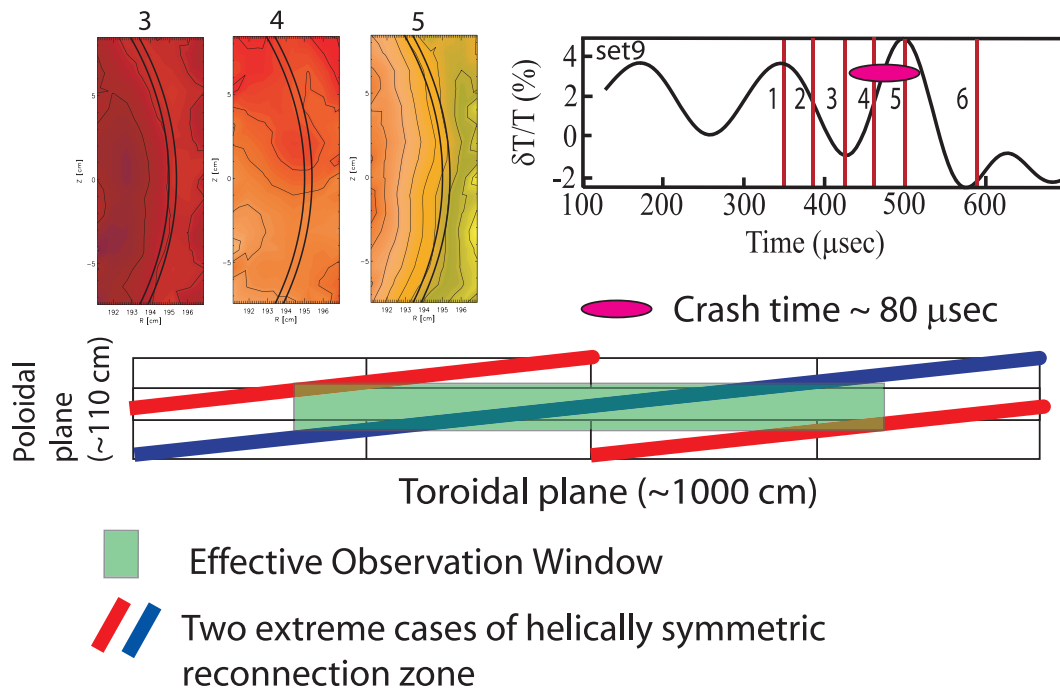


Fig. 5 Effective toroidal window created by the plasma rotation is illustrated on two dimensional space (poloidal and toroidal). Even the worst case of a helically symmetric reconnection zone (width of  $\sim 15$  cm) is overlapping with the window. During the crash time, the window captures only the lower part of the reconnection zone in the 2D data. Approximately one third of the data does not show the reconnection zone during the crash time. Color scale is the same as in Fig. 2.

the inversion radius and the final time when the heat has been migrated to the outside of the inversion radius. Thus, a conservative crash time could be approximately  $\sim 90 \mu\text{s}$  and the toroidal extent of the window becomes approximately  $\sim 650$  cm wide. Even though the vertical view of the image is  $\sim 16$  cm, the effective opening along the inversion radius can be  $\sim 30$  cm, since the direction of the escaping heat can be detected along the upper and lower part of the radial windows.

In Fig. 5, the poloidal and toroidal extent of the window is mapped onto the two dimensional space spanned by the poloidal and toroidal surface of the inversion radius together with two extreme examples of helically symmetric reconnection zones. In the worst case of the helically symmetric reconnection zone, a brief view ( $\sim 13 \mu\text{s}$ ) of the reconnection zone (overlapping zones between red and green color in Fig. 5) in the upper and lower sides of the window. The images in Fig. 5 only captured the reconnection zone for a brief moment ( $\sim 20 \mu\text{s}$ ) at the lower part of the window, while images in Fig. 2 capture most of the reconnection process. For every single crash event, the reconnection zone should be captured by the extended window view and the captured 2-D image can thus range from a partial view for a brief moment to a full view for the entire crash time ( $\sim 90 \mu\text{s}$ ) in the case of a helically symmetric reconnection process. Statistically, one third of the total observed crash events ( $\sim 40$ ) for the window shown in Figs. 2 and 5 did not observe any signature of reconnection zone before the heat is accumulated in the mixing zone. This ob-

servaion can be explained only if the reconnection zone is not helically symmetric. Randomness of the partial view of the reconnection zone when it was captured in the image suggests that the reconnection process must be random in toroidal direction and has to be along the helical structure. Therefore, the entire process can be a random 3-D local reconnection process whereas the previously proposed one is 3-D local reconnection that is confined at the low field side. Furthermore the extent of the reconnection zone is estimated as a  $\sim 1/3$  of the total toroidal length.

## 4. Conclusion

In this review, visualization of the reconnection process of the sawtooth oscillation has significantly improved the understanding of the complexity of the physics of the sawtooth oscillation through comparative study with the prominent theoretical models. The study suggests that the common cause of the reconnection process is a pressure driven mode in both the kink and tearing type of the sawtooth oscillation and that an alternative pressure driven type of mode which can lead to the rupture of the magnetic surface along the inversion radius without preference of magnetic field sides should be considered. The toroidal localization of the reconnection zone is demonstrated to be random along the helical inversion radius and it differs from the earlier 3-D local reconnection model in which the reconnection zone is confined to the lower field side only.

## Acknowledgement

This work is supported by the US DOE contract Nos. DE-AC02-76-CH0-3073, DE-FG03-95ER-54295 and W-7405-ENG-48 and NWO and EURATOM.

- [1] H. Park *et al.*, *Rev. Sci. Instrum.* **75**, 3875 (2004).
- [2] F. Porcelli *et al.*, *Nucl. Fusion* **44**, 362 (2004).
- [3] B.B. Kadomtsev, *Sov. J. Plasma Phys.* **1**, 389 (1975).
- [4] A. Sykes and J.A. Wesson, *Phys. Rev. Lett.* **37**, 140, (1976).
- [5] J.A. Wesson, *Plasma Phys. Control. Fusion* **28**, 243 (1986).
- [6] W. Park *et al.*, *Phys. Rev. Lett.* **75**, 1763 (1995).
- [7] Y. Nishimura, J.D. Callen and C.C. Hegna, *Phys. of Plasmas* **6**, 4685 (1999).
- [8] I. Hutchinson (Cambridge University, New York, 1987).
- [9] G. Bekefi (Wiley, New York, 1966).
- [10] H. Park *et al.*, *Rev. Sci. Instrum.* **74**, 4239 (2003).
- [11] H. Park *et al.*, *Phys. Rev. Lett.* **96**, 195003 (2006).
- [12] H. Park *et al.*, *Phys. Rev. Lett.* **96**, 1950034 (2006).
- [13] H. Park *et al.*, *Phys. of Plasmas* **13**, 055907 (2006).
- [14] W. Park, D.A. Monticello, E. Fredrickson and K. McGuire, *Phys. Fluids B* **3** 507, (1991).
- [15] Y. Nagayama, M. Yamada, W. Park, E.D. Fredrickson, A.C. Janos, K.M. McGuire and G. Taylor, *Phys. Plasma* **3**, 1647 (1996).
- [16] H. Soltwisch, *Rev. Sci. Instrum.* **70**, 815 (1988).
- [17] F.M. Levinton, L. Zakarov, S.H. Batha, J. Manickam and M.C. Zarnstorff, *Phys. Fluids B* **5**, 2554 (1993).